

A superhydrophobic zeolitic imidazolate framework (ZIF-90) with high steam stability for efficient recovery of bioalcohols[†]

Chuanyao Liu, Qian Liu and Aisheng Huang*

A superhydrophobic zeolitic imidazolate framework (ZIF-90) with high steam stability is prepared through post-functionalization *via* an amine condensation reaction. The developed superhydrophobic ZIF-90 is highly promising as an effective and reusable adsorbent for bio-alcohol recovery.

Due to the emerging scarcity of fossil resources and critical environment concerns, the development of renewable and clean energy sources such as bioalcohols has drawn increasing interest in recent years.¹ Bioalcohols are usually produced from biomass through fermentation with a low alcohol concentration in an aqueous medium. Therefore, it is a prerequisite to extract and recover the bioalcohol from the fermentation broth before it can be used as a biofuel. Distillation is a conventional technology for the separation of an alcohol/water mixture. However, it involves high energy consuming boiling and condensing processes. Adsorptive separation using porous materials is regarded as one of the most competitive methods as it is energy-saving and environmentally friendly. So far, various materials including activated carbons, polymeric resins and zeolites have been developed for the separation of alcohol/water mixtures.²⁻⁶ However, these adsorbents have a strong affinity to water, resulting in a low adsorption capacity and effectiveness. Therefore, the development of a novel adsorbent with high adsorption performance remains an urgent challenge.

In the past ten years, metal–organic frameworks (MOFs) have received considerable interest because of their potential applications in gas adsorption and storage, membrane separation, chemical sensors, and drug delivery.⁷⁻¹² In particular, zeolitic imidazolate frameworks (ZIFs), a subfamily of MOFs based on transition metals and imidazolate linkers,^{13,14} have emerged as a novel type of porous material for the fabrication of molecular sieving

membranes due to their zeolite-like properties such as permanent porosity, uniform pore size, and exceptional thermal and chemical stability.¹⁵⁻²¹ Furthermore, ZIFs are also promising adsorbents for the recovery of bio-alcohols due to their tunable pore size and adjustable internal surface properties.^{22,23} It is well recognized that the adsorption performances of the adsorbents are determined not only by their open pore structures and surface areas, but also their hydrophobicity.^{3,24} Therefore, the development of superhydrophobic adsorbents with open pore structures, high stability and large surface areas is of special interest. To the best of our knowledge, so far no studies on the synthesis and application of superhydrophobic ZIFs have been reported.

Recently, Yaghi and co-workers have developed a novel SOD topology ZIF-90 through a solvothermal reaction of zinc(II) and imidazolate-2-carboxyaldehyde (ICA).²⁵ ZIF-90 shows not only a high stability but also a permanent microporosity with a narrow pore size (~3.5 Å) and high BET surface area (1270 m² g⁻¹). The presence of free aldehyde groups in the ZIF-90 framework allows the covalent functionalization of ZIF-90 with amine groups *via* an imine condensation reaction. Based on the imine condensation reaction, we have developed a covalent post-functionalization strategy to enhance the molecular sieve performances of the ZIF-90 membrane.^{26,27} Indeed, the postsynthetic modification of MOFs is well known as an effective and versatile strategy to improve the physical and chemical properties.²⁸⁻³² Due to the presence of the free aldehyde groups in the ZIF-90 framework, ZIF-90 is an ideal candidate for the post-functionalization through host–guest reactions, generating a large number of topologically identical but functionally diverse ZIF-90 with fine-tuned and optimized properties.²⁵⁻²⁹ In the present work, we report the synthesis of a superhydrophobic ZIF-90 for bioalcohol recovery through the post-functionalization of ZIF-90 with pentafluorobenzylamine *via* an amine condensation reaction (Fig. 1 and Fig. S1, ESI[†]). It is expected that the fluorinated ZIF-90 will show a high hydrophobicity and thus is promising for bioalcohol recovery.

Pentafluorobenzylamine was synthesized according to a procedure reported elsewhere with minor modification (Fig. S2, the details see ESI[†]).³³ The formation of pentafluorobenzylamine

Institute of New Energy Technology, Ningbo Institute of Material Technology and Engineering, CAS, 1219 Zhongguan Road, 315201 Ningbo, P. R. China.
E-mail: huangaisheng@nimte.ac.cn

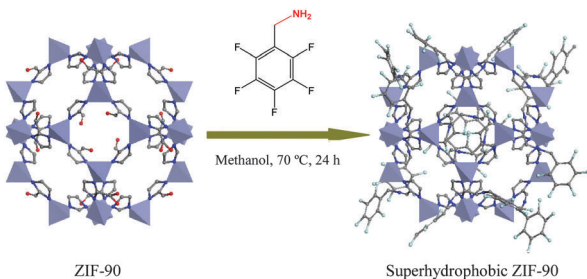


Fig. 1 Scheme of the synthesis of superhydrophobic ZIF-90 via an amine condensation reaction.

is confirmed by Fourier transform infrared (FT-IR) and $^1\text{H-NMR}$ nuclear magnetic resonance (NMR) spectra (Fig. S3, ESI \dagger). The ZIF-90 was prepared by a solvothermal reaction of zinc(II) nitrate tetrahydrate, sodium formate, and ICA in methanol.³⁴ As shown in Fig. 2a, well-defined ZIF-90 crystals with a dodecahedral morphology and size of about $2.0 \pm 0.5 \mu\text{m}$ are prepared after solvothermal synthesis for 24 h at 85 °C. For the covalent post-functionalization, the as-prepared ZIF-90 crystals were immersed in a solution of pentafluorobenzylamine in methanol, and then refluxed for 24 h at 70 °C. The post-functionalization of ZIF-90 with pentafluorobenzylamine was confirmed by FT-IR spectroscopy and X-ray photoelectron spectroscopy (XPS). As shown in Fig. S4 (ESI \dagger), the C=O band of the aldehyde at 1678 cm $^{-1}$ is replaced by the C=N bond of the imine at 1630 cm $^{-1}$. The presence of an aromatic C-C band at 1510 cm $^{-1}$ and F-C bands at 1030, 1125, and 1235 cm $^{-1}$ suggests that pentafluorobenzylamine has been grafted on the ZIF-90 after post-modification. As shown in Fig. S5 and Table S1 (ESI \dagger), after post-modification, the intensity of the O 1s and Zn 2p peaks reduces greatly and a new F 1s peak emerges with a high intensity, confirming that pentafluorobenzylamine has successfully reacted with the aldehyde groups of ZIF-90. Since the kinetic diameters of pentafluorobenzylamine are much larger than the pore size of ZIF-90, it is difficult for pentafluorobenzylamine to go into the ZIF-90 cage. Therefore, the post-synthetic modification

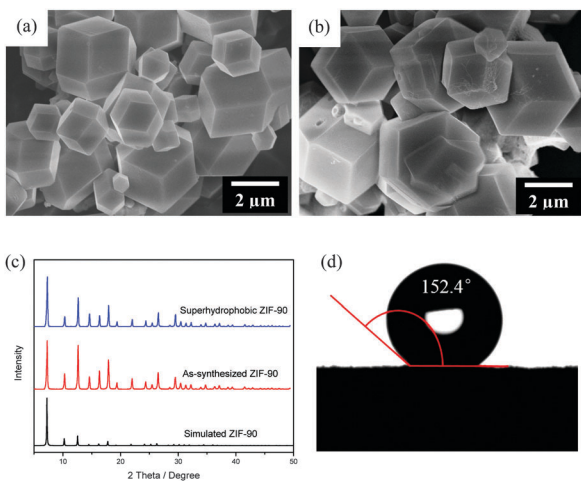


Fig. 2 FESEM images of ZIF-90 (a) and superhydrophobic ZIF-90 (b), XRD patterns of ZIF-90 and superhydrophobic ZIF-90 (c), and measurement of the contact angle with water for the superhydrophobic ZIF-90 (d).

reaction mainly occurs at the external surface of the ZIF-90 particles, as shown in Fig. S6 (ESI \dagger).³⁵ The successful post-functionalization of ZIF-90 was further confirmed by N₂ adsorption isotherms. As shown in Fig. S7a (ESI \dagger), the N₂ adsorption isotherm for ZIF-90 showed a steep rise in the low-pressure region, indicating the permanent porosity of the ZIF-90 framework.²⁵ The calculated BET surface area of ZIF-90 in the present work is about 1182 m 2 g $^{-1}$, which is in good agreement with the previous report.²⁵ However, after post-functionalization, the pore aperture of the fluorinated ZIF-90 is severely constricted, leading to a low N₂ adsorption (Fig. S7b, ESI \dagger).

After post-functionalization, no remarkable differences in the ZIF-90 morphology are found between the as-prepared and the fluorinated ZIF-90 (Fig. 2b). As deduced from the X-ray diffraction (XRD) pattern (Fig. 2c), the high crystallinity of the ZIF-90 structure remains unchanged after post-modification, even after being boiled in water for 24 h (Fig. S8, ESI \dagger). Furthermore, from the thermogravimetric analysis (TGA) (Fig. S9, ESI \dagger), both the as-prepared and fluorinated ZIF-90 show a similar plateau region without a significant weight loss in the temperature range of 80–300 °C, even after the measurement of the water stability (Fig. S10, ESI \dagger). These results indicate that the fluorinated ZIF-90 shows a high thermal and chemical stability.

The hydrophobicity of the fluorinated ZIF-90 was evaluated by measurement of the water contact angle (CA). As shown in Fig. 2d, the surface of the fluorinated ZIF-90 shows a water CA of about 152.4°, while the water CA of the surface of the as-prepared ZIF-90 is 93.9° (Fig. S11, ESI \dagger), suggesting that the hydrophobicity of the ZIF-90 can be significantly enhanced through post-functionalization with pentafluorobenzylamine. Such a surface superhydrophobicity should be attributed to the cooperation of both the microporous morphological structures and strongly hydrophobic chemical compositions of the fluorinated ZIF-90, which are two well-known key factors for the surface superhydrophobicity.^{24,36}

The hydrophobicity of the fluorinated ZIF-90 was further confirmed by the removal of alcohols from alcohol/water mixtures. To evaluate the adsorption capacity of the fluorinated ZIF-90 for the recovery of alcohols from alcohol/water mixtures, the superhydrophobic ZIF-90 powders were added into an ethanol/water mixture which was dyed with red oil for clarity, and then kept stirring for 2 h. After selective adsorption of ethanol for 20 h, the fluorinated ZIF-90 powders which had adsorbed ethanol were separated by a simple filtration. As shown in Fig. S12c (ESI \dagger), the mother solution becomes colourless and transparent after the removal of the fluorinated ZIF-90 powders by filtration, indicating that ethanol has been fully recovered and removed by the fluorinated ZIF-90. Indeed, according to the analysis of the gas chromatograph (GC), 98% ethanol has been removed from the ethanol/water mixture (Fig. 3). On the contrary, only 7% ethanol can be removed from the ethanol/water mixture when using the as-prepared ZIF-90 as the adsorbent (Fig. S13, ESI \dagger). Besides ethanol, the superhydrophobic ZIF-90 also displays high adsorptive separation performances for the removal of other bioalcohols such as methanol, iso-propanol and butanol, as well as its mixtures (Fig. 3). Furthermore, the superhydrophobic ZIF-90 can be easily regenerated by a simple thermal regeneration under

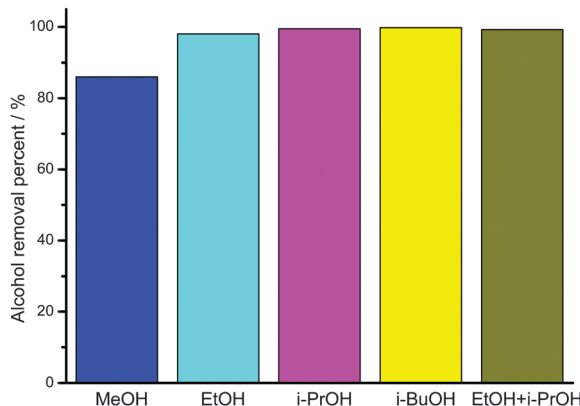


Fig. 3 Adsorptive separation performance of the superhydrophobic ZIF-90 for the removal of alcohols from alcohol/water mixtures.

vacuum at 65 °C, and the superhydrophobic ZIF-90 is still highly active after five successive cycles of separation due to its high stability, with an almost constant alcohol removal percentage (Fig. S13, ESI[†]). From the TGA measurement of the superhydrophobic ZIF-90 which has fully adsorbed ethanol, a similar plateau region without a significant weight loss in the temperature range of 80–300 °C is still observed, and the initial weight loss is about 20% at 30–80 °C due to the release of ethanol (Fig. S14, ESI[†]). These results are in good agreement with our supposition that the superhydrophobic ZIF-90 is very promising for use as an effective and reusable adsorbent for bio-alcohol recovery from aqueous solutions.

In conclusion, based on an amine condensation reaction between the aldehyde groups of ZIF-90 and amine groups of pentafluorobenzylamine, we have developed a facile post-functionalization route for the preparation of superhydrophobic ZIF-90. After post-functionalization, the water CA can be enhanced from 93.9° to 152.4°, while both the dodecahedral morphology and SOD structure of ZIF-90 remain unchanged due to its high stability. The developed superhydrophobic ZIF-90 displays a high adsorptive separation performance for the recovery of bio-alcohols. At 20 °C, more than 98% bio-alcohol (ethanol, iso-propanol and butanol) can be recovered and removed from the bio-alcohol/water mixture. These properties present the superhydrophobic ZIF-90 as a promising candidate for industrial bio-alcohol recovery.

This work was financially supported by the Ningbo Science and Technology Innovation Team (2014B81004), and Ningbo Municipal Natural Science Foundation (2015A610046).

References

- 1 J. A. Turner, *Science*, 1999, **285**, 687–689.
- 2 S. J. T. Pollard, G. D. Fowler, C. J. Sollars and R. Perry, *Sci. Total Environ.*, 1992, **116**, 31–52.
- 3 A. Li, H. X. Sun, D. Z. Tan, W. J. Fan, S. H. Wen, X. J. Qing, G. X. Li, S. Y. Li and W. Q. Deng, *Energy Environ. Sci.*, 2011, **4**, 2062–2065.
- 4 T. Ono, T. Sugimoto, S. Shinkai and K. Sada, *Nat. Mater.*, 2007, **6**, 429–433.
- 5 K. Zhang, R. P. Lively, J. D. Noel, M. E. Dose, B. A. McCool, R. R. Chance and W. J. Koros, *Langmuir*, 2012, **28**, 8664–8673.
- 6 K. Zhang, R. P. Lively, M. E. Dose, L. Li, W. J. Koros, D. M. Ruthven, B. A. McCool and R. R. Chance, *Microporous Mesoporous Mater.*, 2013, **170**, 259–265.
- 7 R. Banerjee, A. Phan, B. Wang, C. Knobler, H. Furukawa, M. O’Keeffe and O. M. Yaghi, *Science*, 2008, **319**, 939–943.
- 8 B. Wang, A. P. Cote, H. Furukawa, M. O’Keeffe and O. M. Yaghi, *Nature*, 2008, **453**, 207–211.
- 9 H. T. Kwon and H. K. Jeong, *J. Am. Chem. Soc.*, 2013, **135**, 10763–10768.
- 10 A. R. Millward and O. M. Yaghi, *J. Am. Chem. Soc.*, 2005, **127**, 17998–17999.
- 11 G. Lu and J. T. Hupp, *J. Am. Chem. Soc.*, 2010, **132**, 7832–7833.
- 12 Y. Lee, S. Kim, J. K. Kang and S. M. Cohen, *Chem. Commun.*, 2015, **51**, 5735–5738.
- 13 K. S. Park, Z. Ni, A. P. Cote, J. Y. Choi, R. Huang, F. J. Uribe-Romo, H. K. Chae, M. O’Keeffe and O. M. Yaghi, *Proc. Natl. Acad. Sci. U. S. A.*, 2006, **103**, 10186–10191.
- 14 X. C. Huang, Y. Y. Lin, J. P. Zhang and X. M. Chen, *Angew. Chem., Int. Ed.*, 2006, **45**, 1557–1559.
- 15 H. Bux, F. Liang, Y. Li, J. Cravillon, M. Wiebcke and J. Caro, *J. Am. Chem. Soc.*, 2009, **131**, 16000–16001.
- 16 Y. S. Li, F. Y. Liang, H. Bux, A. Feldhoff, W. S. Yang and J. Caro, *Angew. Chem., Int. Ed.*, 2010, **49**, 548–551.
- 17 Y. Pan and Z. Lai, *Chem. Commun.*, 2011, **47**, 10275–10277.
- 18 A. Huang, Y. Chen, N. Wang, Z. Hu, J. Jiang and J. Caro, *Chem. Commun.*, 2012, **48**, 10981–10983.
- 19 Z. Xie, J. Yang, J. Wang, J. Bai, H. Yin, B. Yuan, J. Lu, Y. Zhang, L. Zhou and C. Duan, *Chem. Commun.*, 2012, **48**, 5977–5979.
- 20 A. Huang, Q. Liu, N. Wang, Y. Zhu and J. Caro, *J. Am. Chem. Soc.*, 2014, **136**, 14686–14689.
- 21 A. Huang, W. Dou and J. Caro, *J. Am. Chem. Soc.*, 2010, **132**, 15562–15564.
- 22 K. Zhang, R. P. Lively, M. E. Dose, A. J. Brown, C. Zhang, J. Chung, S. Nair, W. J. Koros and R. R. Chance, *Chem. Commun.*, 2013, **49**, 3245–3247.
- 23 K. Zhang, K. M. Gupta, Y. Chen and J. Jiang, *AIChE J.*, 2015, **61**, 2763–2775.
- 24 X. Yao, Y. Song and L. Jiang, *Adv. Mater.*, 2011, **23**, 719–734.
- 25 W. Morris, C. J. Doonan, H. Furukawa, R. Banerjee and O. M. Yaghi, *J. Am. Chem. Soc.*, 2008, **130**, 12626–12627.
- 26 A. Huang and J. Caro, *Angew. Chem., Int. Ed.*, 2011, **50**, 4979–4982.
- 27 A. Huang, N. Wang, C. Kong and J. Caro, *Angew. Chem., Int. Ed.*, 2012, **51**, 10551–10555.
- 28 H. Li, X. Feng, Y. Guo, D. Chen, R. Li, X. Ren, X. Jiang, Y. Dong and B. Wang, *Sci. Rep.*, 2014, **4**, 4366.
- 29 A. Karmakar, N. Kumar, P. Samanta, A. V. Desai and S. K. Ghosh, *Chem. – Eur. J.*, 2015, **3**, 1521–3765.
- 30 Z. Wang and S. M. Cohen, *J. Am. Chem. Soc.*, 2007, **129**, 12368–12369.
- 31 E. Dugan, Z. Wang, M. Okamura, A. Medina and S. M. Cohen, *Chem. Commun.*, 2008, 3366–3368.
- 32 T. Gadzikwa, G. Lu, C. L. Stern, S. R. Wilson, J. T. Hupp and S. T. Nguyen, *Chem. Commun.*, 2008, 5493–5495.
- 33 B. Kumar Das, N. Shibata and Y. Takeuchi, *J. Chem. Soc., Perkin Trans. 1*, 2002, 197–206.
- 34 Q. Liu, N. Wang, J. Caro and A. Huang, *J. Am. Chem. Soc.*, 2013, **135**, 17679–17682.
- 35 X. Liu, Y. Li, Y. Ban, Y. Peng, H. Jin, H. Bux, L. Xu, J. Caro and W. Yang, *Chem. Commun.*, 2013, **49**, 9140–9142.
- 36 L. Gao and T. J. McCarthy, *J. Am. Chem. Soc.*, 2006, **128**, 9052–9053.

Supplemental Information

Superhydrophobic Zeolitic Imidazolate Framework ZIF-90 with High Steam Stability for Efficient Recover of Bioalcohols

Chuanyao Liu, Qian Liu, and Aisheng Huang

Institute of New Energy Technology, Ningbo Institute of Material Technology and Engineering, CAS,
1219 zhongguan Road, 315201 Ningbo, P. R. China

Experimental details:

Chemicals were used as received: Imidazolate-2-carboxyaldehyde (ICA, >99%, Alfa Aesar), Zn(NO₃)₂·6H₂O (>99%, Merck), sodium formate (99.99% metals basis, Aladdin), methanol (>99.5%, Sinopharm Chemical Reagent Co. Ltd), diethyl ether (>99.7, Sinopharm Chemical Reagent Co. Ltd), 2,3,4,5,6-Pentafluorobenzonitrile (>99%, Sigma-Aldrich), BH₃·THF (1.0 M, Sigma-Aldrich), THF (anhydrous, >99.9%, Sigma-Aldrich), HCl (>99%, Aladdin), NaOH (>97%, Aladdin), Na₂SO₄ (>99%, Aladdin), ethanol (>97%, Aladdin).

Preparation of pentalfluorobenzylamine: Pentalfluorobenzylamine was synthesized according to the chemical reaction shown in **Fig. S2** with the procedure reported elsewhere with minor modification.¹ Typically, BH₃·THF (1 M; 25 ml, 25 mmol) was carefully added into pentafluorobenzonitrile (1 g, 5.18 mmol) anhydrous THF (80 ml) solution in a round bottom flask at 293 K under stirring condition. Then the resulting mixture was refluxed (373 K) and stirred for 10 h. After reaction, the mixture was cooled to 273 K, and 2.6 M HCl (100 ml) was carefully added into the mixture. And then, the resulting mixture was continued to reflux for 1 h. The resultant solution was evaporated under vacuum to remove THF with conventional rotary evaporation method. Excessive HCl solution was added to the residue and then extracted with diethyl ether (200 ml) for 3 times. The water phase was treated with 10% NaOH aqueous until the pH reached to 10 ~ 11, and then extracted with excessive diethyl ether (100 ml) for 3 times. The combined organic phase was washed thoroughly with sodium chloride solution, and then dried over with Na₂SO₄. The solvent was removed under vacuum and light yellow liquid was obtained, which was used without further purification. The formation of pentalfluorobenzylamine was confirmed by fourier transform infrared (FT-IR) spectroscopy and ¹H-NMR nuclear magnetic resonance (NMR) spectroscopy. The FT-IR spectroscopy was achieved in the absorbance mode in a Bruker Tensor 27 spectro photometer. The NMR spectroscopy was obtained at ambient temperature using a Bruker 400 MHz instrument (NMR

Switzerland Bruker 400MHz AVANCE III). The signals are presented relative to TMS as 0 ppm, and CDCl₃ was used for solvent.

Synthesis of ZIF-90: ZIF-90 crystals were synthesized by solvothermal method in a Teflon-lined autoclave according to the procedure reported elsewhere.² Normally, a solid mixture of 0.296 g (1.00 mmol) zinc nitrate hexahydrate, 0.384 g (4.00 mmol) imidazole-2-formaldehyde and 0.068 g (1.00 mmol) sodium formate was dissolved in 40 ml methanol by ultrasonic treatment. The as-prepared solution was placed in a Teflon-lined stainless steel autoclave, and heated at 85 °C in an air-circulating oven for 24 h. After solvothermal reaction and cooling to 20 °C, the ZIF-90 crystals was filtered and washed with methanol three times, and then dried in air for 24 h at room temperature.

Synthesis of superhydrophobic ZIF-90: The as-synthesized ZIF-90 crystals (0.15 g, 0.59 mmol) and 10 mL pentafluorobenzylamine (0.347g, 1.76 mmol) were suspended in methanol solution, and refluxed at 100 °C for 24 h. And then the solid was filtered and washed with fresh methanol (20 mL) three times to obtain superhydrophobic ZIF-90 crystals. Finally, the superhydrophobic ZIF-90 crystals were dried under vacuum (10⁻² Torr) for 24 h at room temperature.

Characterization of as-synthesized ZIF-90 and superhydrophobic ZIF-90: The morphology of the as-synthesized ZIF-90 and superhydrophobic ZIF-90 was characterized by field emission scanning electron microscopy (FESEM). FESEM micrographs were taken on an S-4800 (Hitachi) with a cold field emission gun operating at 4 kV and 10 μA. The phase purity and crystallinity of the as-synthesized ZIF-90 and superhydrophobic ZIF-90 was confirmed by X-ray diffraction (XRD). The XRD patterns were recorded at room temperature under ambient conditions with Bruker D8 ADVANCE X-ray diffractometer with Cu Kα radiation at 40 kV and 40 mA. FT-IR spectra of the as-synthesized ZIF-90 and superhydrophobic ZIF-90 were obtained by using Bruker TENSOR27 Impact spectrometer. The superhydrophobic performance of the as-synthesized ZIF-90 and superhydrophobic ZIF-90 was evaluated by water contact angle (CA). The water contact angle was measured with a Dataphysics OCA20 contact-angle system at room temperature under ambient conditions. Water droplets (about 5 μL) were dropped

carefully onto the surface of the as-synthesized ZIF-90 and superhydrophobic ZIF-90 crystals. The contact angle value for each sample was obtained by measuring four different positions of the same sample and averaging them to get the final contact angle value.

Thermal and hydrothermal stability measurement of the as-synthesized ZIF-90 and superhydrophobic ZIF-90: The thermal stability of the as-synthesized ZIF-90 and superhydrophobic ZIF-90 was measured by Thermogravimetric analyses (TGA). TGA was carried out using a Mettler Toledo TGA/STDA 851e. Samples (10 mg) placed in 70 μL alumina pans were heated in an air flow from 0 to 900 $^{\circ}\text{C}$ with a heating rate of 5 $^{\circ}\text{C}/\text{min}$.

The as-synthesized ZIF-90 and fluorinated ZIF-90 crystals were boiled in water for testing their thermal stability. The as-synthesized ZIF-90 and fluorinated ZIF-90 crystals (0.06 g) were respectively added into water (1 g), and then were placed in a Teflon-lined stainless steel autoclave and heated at 100 $^{\circ}\text{C}$ in an air-circulating oven for 24 h. After the treatment in boilling water, the as-prepared ZIF-90 and fluorinated ZIF-90 crystals were separated by filtration.

Adsorptive separation of alcohols/water mixture by using the as-synthesized ZIF-90 and superhydrophobic ZIF-90: To evaluate the adsorption capacity of the as-synthesized ZIF-90 and superhydrophobic ZIF-90 for the recovery of alcohols from alcohol/water mixtures, the as-synthesized ZIF-90 and superhydrophobic ZIF-90 powders (0.2 g) were added into 10 wt% ethanol/water mixture (5.0 g) which was dyed by red oil for clarity, and then keeping stirring for 2 h. After a following selective adsorption of ethanol for 20 h, the as-synthesized ZIF-90 and superhydrophobic ZIF-90 powders which have adsorbed ethanol were separated by a simple filtration. After filtration. the obtained supernatants was analyzed by liquid chromatography to determine the relative content of ethanol. Before and after adding the superhydrophobic ZIF-90 powders, the compositions of the alcohol/water mixture were analyzed by gas chromatography (GC-1690T, Jiedao). The alcohol removal percentage was used to evaluate the adsorptive separation performance of the the superhydrophobic ZIF-90. The alcohol removal percentage was calculated using the following equation:

$$R_{alcohol} = \left(1 - \frac{Wt(alcohol)_{final}}{Wt(alcohol)_{initial}}\right) \times 100\%$$

Where $Wt(alcohol)_{initial}$ and $Wt(alcohol)_{final}$ are the initial alcohol weight and final alcohol weight of the alcohol/water mixture, respectively.

Reference

- 1 B. Kumar Das, N. Shibata and Y. Takeuchi, *J. Chem. Soc. Perkin Trans*, 2002, **1**, 197–206.
- 2 Q. Liu, N. Wang, J. Caro and A. Huang, *J. Am. Chem. Soc.*, 2013, **135**, 17679-17682.

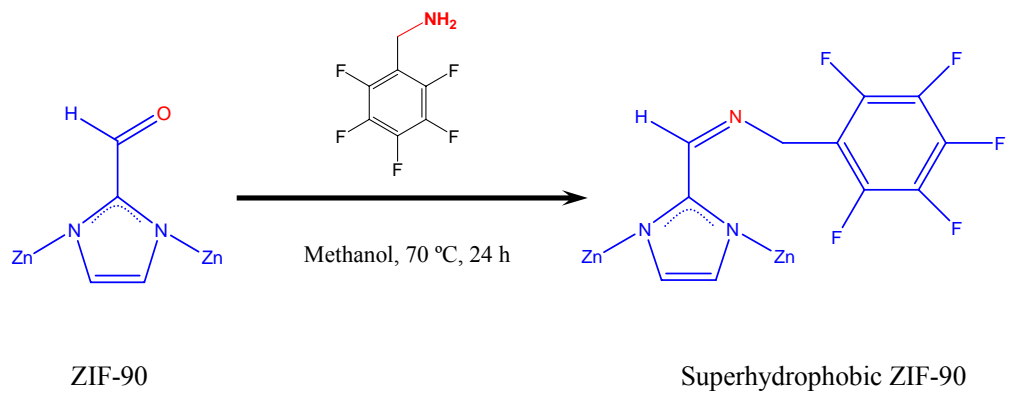


Fig. S1. Schematic diagram of covalent post-functionalization of ZIF-90 via imines condensation reaction to prepare superhydrophobic ZIF-90.

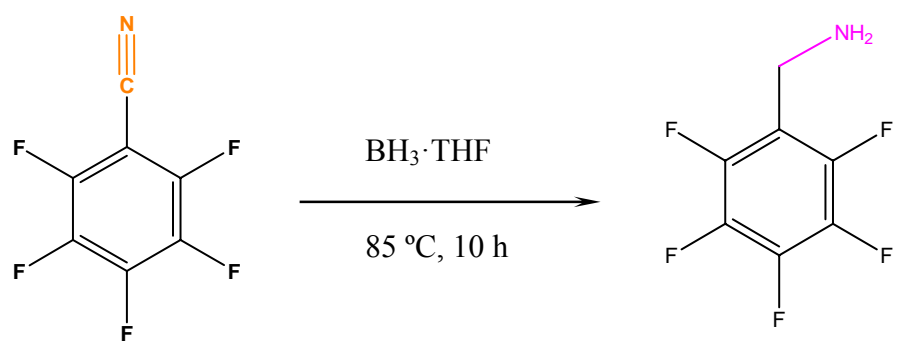


Fig. S2. Schematic diagram of the preparation of pentalfluorobenzylamine.

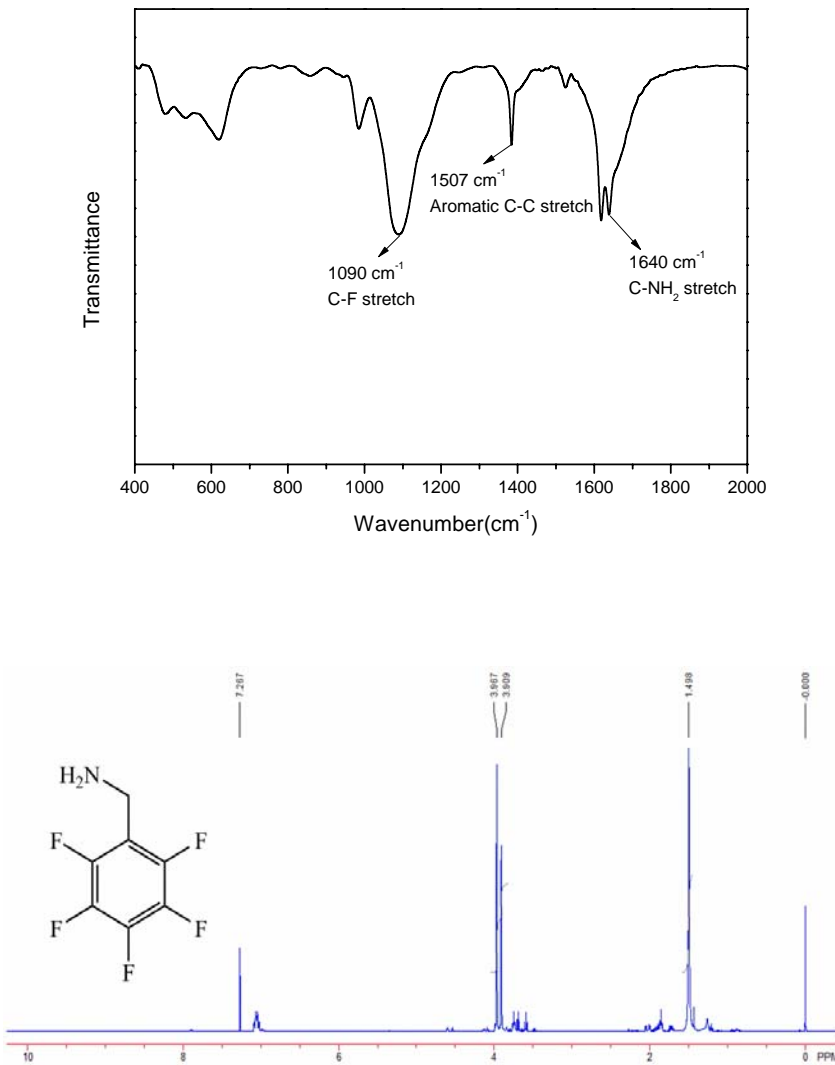


Fig. S3. (a) FT-IR spectra of pentafluorobenzylamine amino stretch at 1640 cm^{-1} , C-F (aromatic) covalent bond at 1100 cm^{-1} highlighted for clarity, (b) ¹H NMR spectrum for the as-synthesized pentafluorobenzylamine (400 MHz, CDCl_3 , 298K, TMS): 7.26 ppm (2H, s, CDCl_3), 3.96 ppm (2H, s, ArCH₂), 1.50 ppm (2H, s).

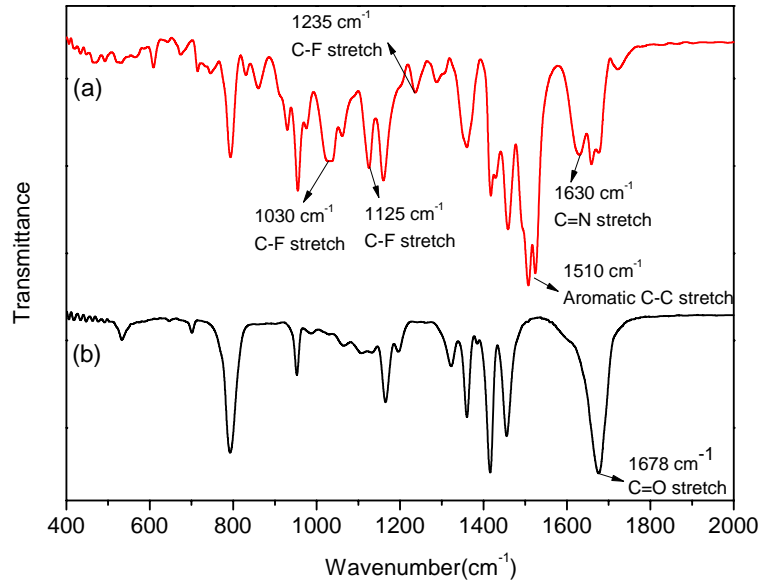


Fig. S4. FT-IR spectrums of the as-prepared ZIF-90 (a) and superhydrophobic ZIF-90 (b).

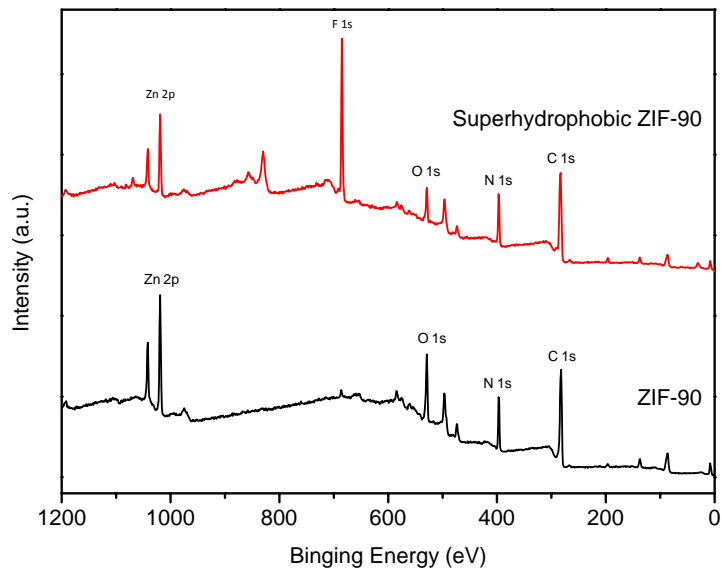


Fig. S5. XPS spectra of the ZIF-90 and superhydrophobic ZIF-90.

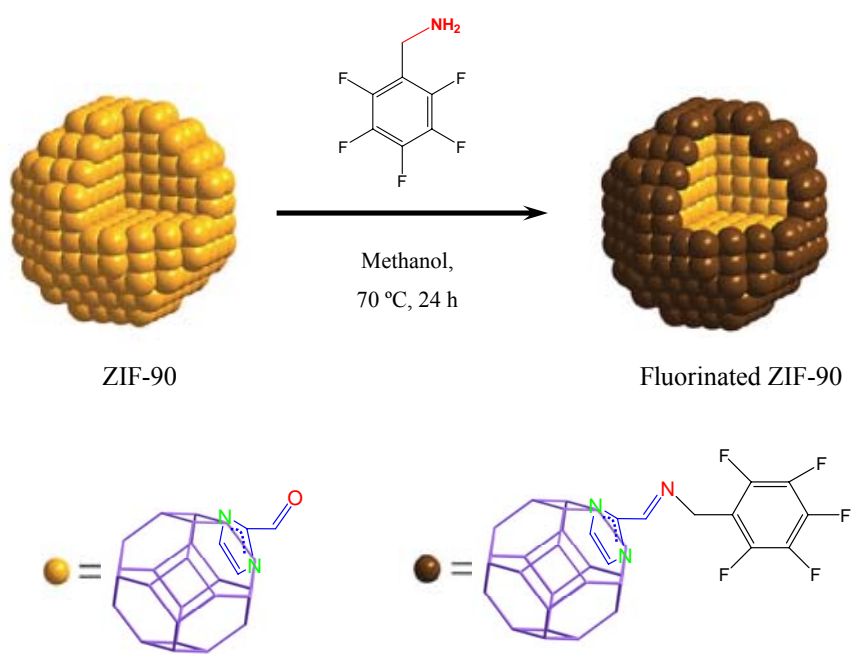


Fig. S6. Schematic diagram of covalent post-functionalization of ZIF-90 at the external surface of ZIF-90 crystals (X. Liu, et al., Chem. Commun., 2013, 49, 9140).

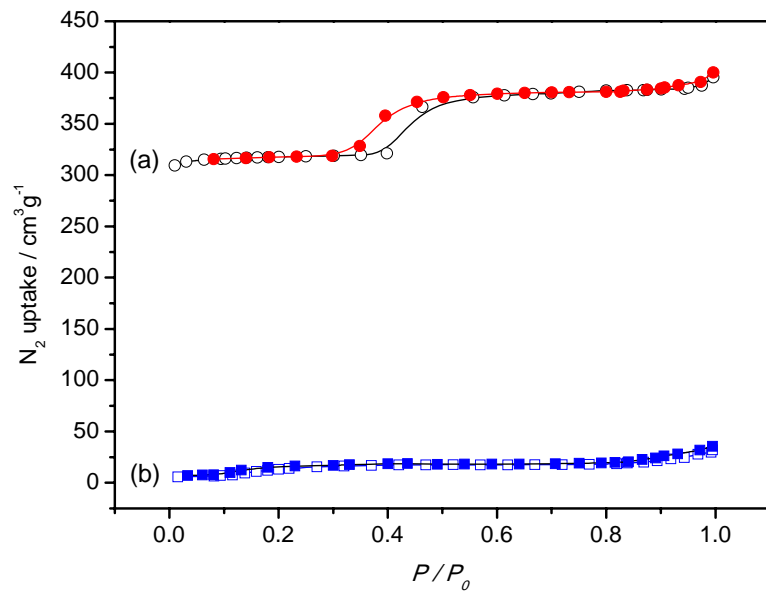


Fig. S7. N₂ isotherms for the as-synthesized ZIF-90 (a) and superhydrophobic ZIF-90 (b) measured at 77 K. Open and filled circles represent adsorption and desorption branch, respectively.

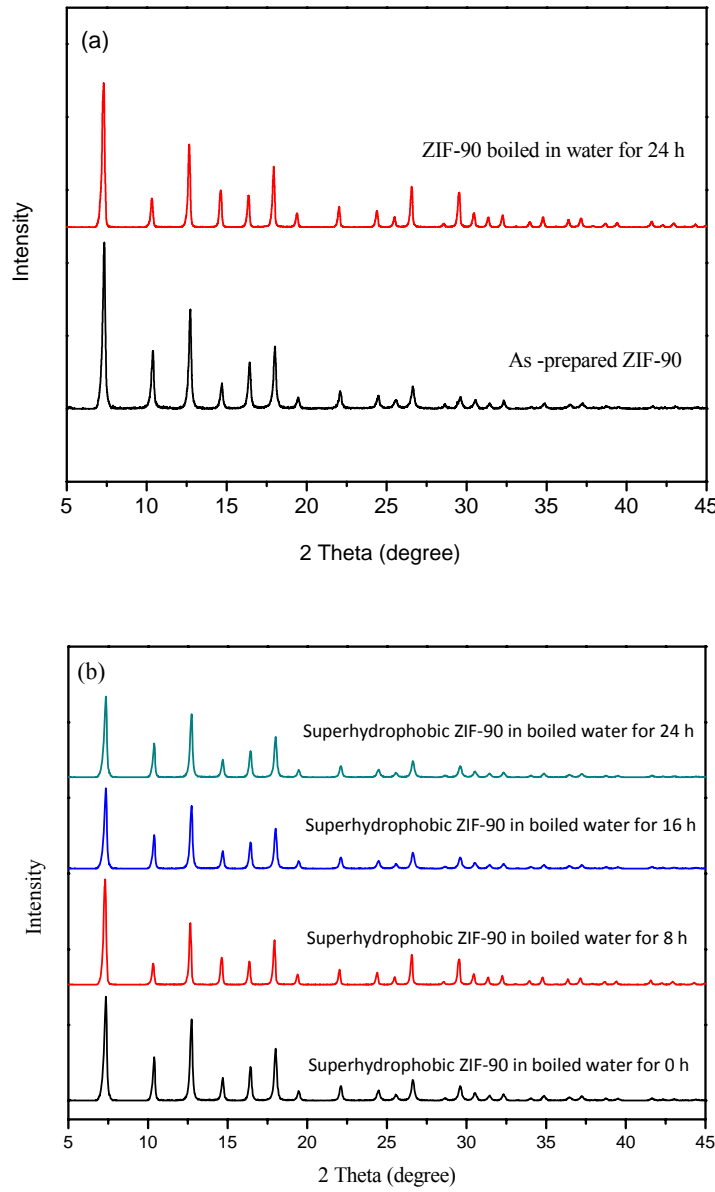


Fig. S8. XRD patterns of the as-prepared ZIF-90 before or after being boiled in water for 24 h (a), and superhydrophobic ZIF-90 after being boiled in water for different time (b).

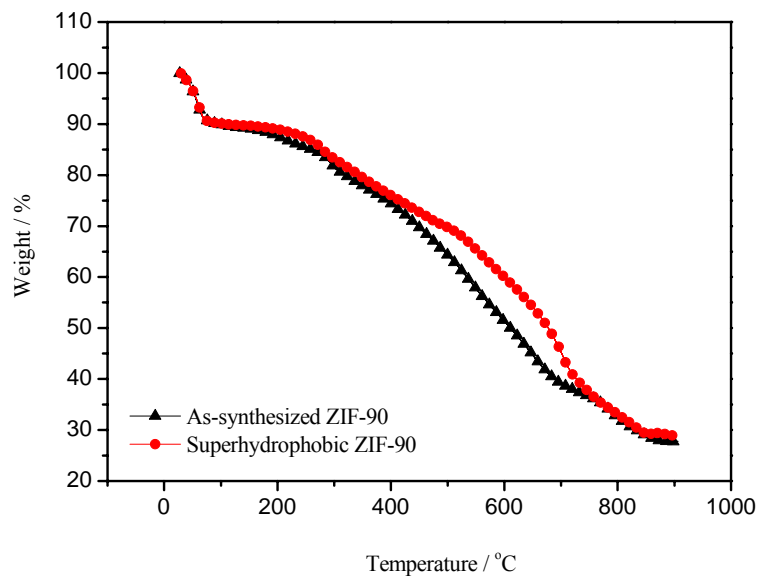


Fig. S9. TGA trace of the as-synthesized ZIF-90 and superhydrophobic ZIF-90. The initial weight loss 30-90 °C is due to methanol trapped within the pores. The loss of weight 20-80 °C is most likely due to strongly associated solvent within the framework.

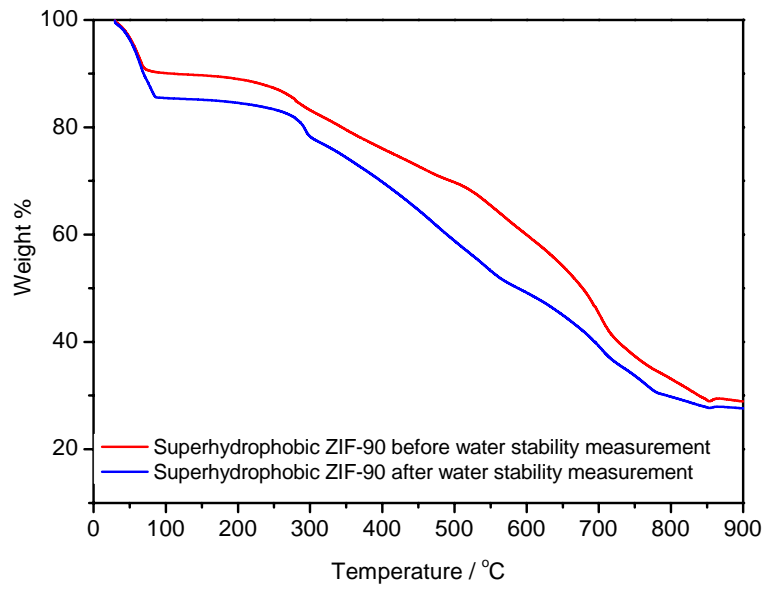


Fig. S10. TGA of the superhydrophobic ZIF-90 before and after the measurement of water stability.

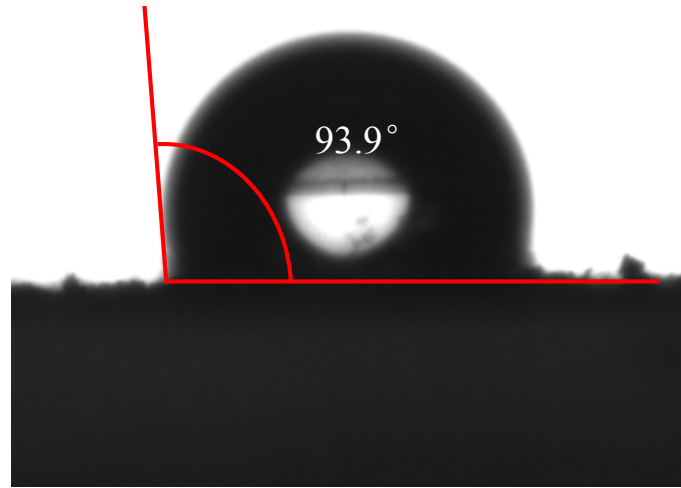


Fig. S11. Measurement of water contact angle (CA) for the as-prepared ZIF-90.

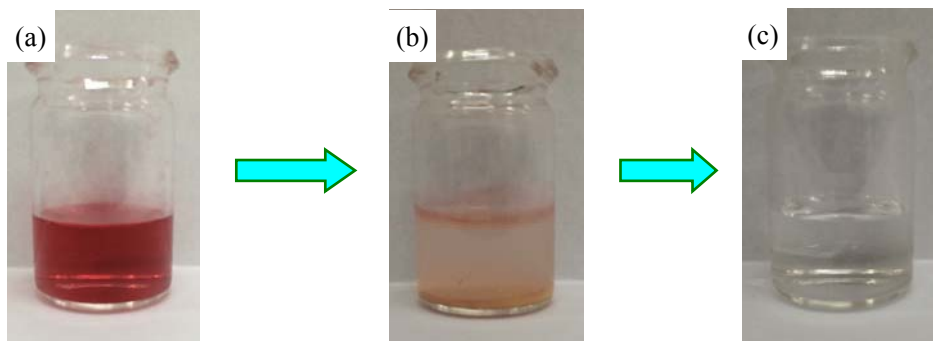


Fig. S12. Snapshots showing the adsorption and removal of ethanol (the ethanol was dyed by red oil for clarity) from 10 wt% ethanol/water solution by using the superhydrophobic ZIF-90. (a) ethanol/water solution before adding the superhydrophobic ZIF-90 particles; (b) ethanol/water solution after adding the superhydrophobic ZIF-90 particles and standing for 20 h at 20 °C; (c) ethanol/water solution after filtering and removing the superhydrophobic ZIF-90 particles which have adsorbed ethanol.

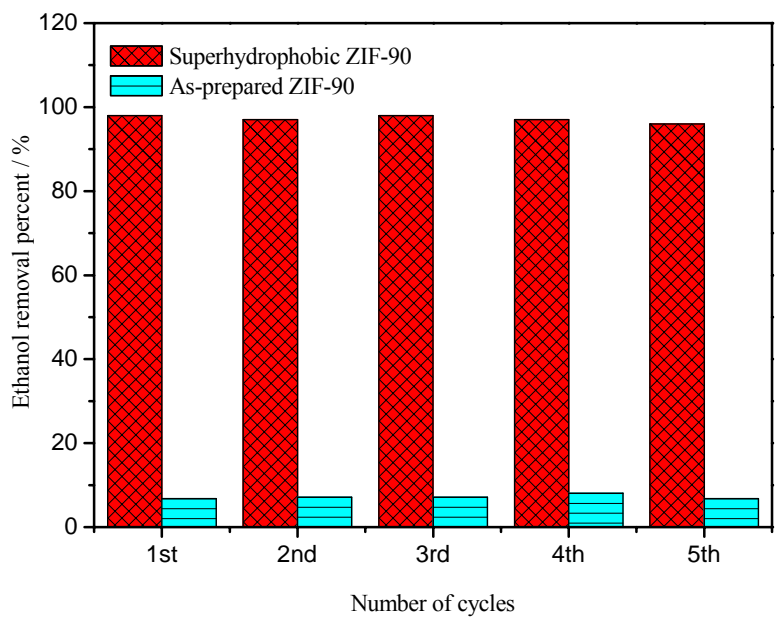


Fig. S13. Comparision of ethanol removal percent between the superhydrophobic ZIF-90 and as-synthesized ZIF-90.

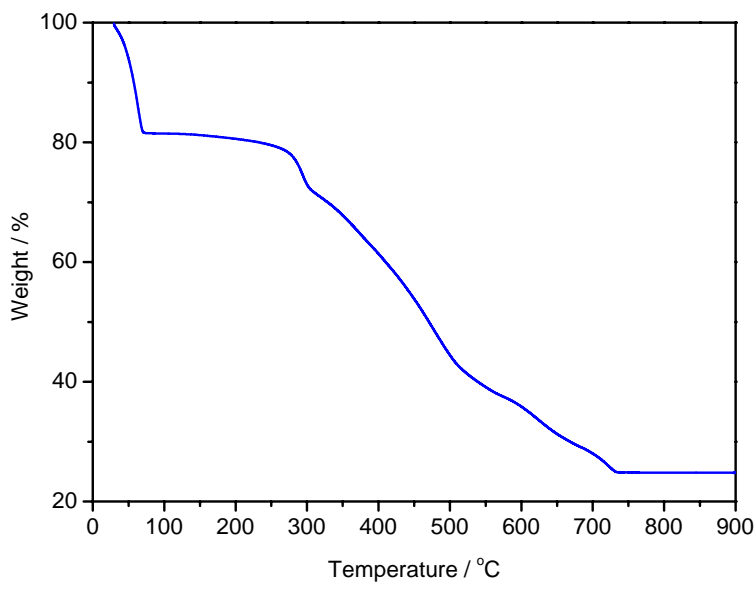


Fig. S14. TGA trace of the superhydrophobic ZIF-90 which has fully adsorbed ethanol.

Table S1**Table S1.** Element composition of the ZIF-90 and superhydrophobic ZIF-90.

Samples	Element composition (Wt%)				
	Zn	F	O	N	C
ZIF-90	23.22	0	15.23	14.55	47
Superhydrophobic ZIF-90	13.87	24.55	5.39	12.78	43.4